Chemistry and Physics of Lipids 163 (2010) 182–189

Contents lists available at ScienceDirect

Chemistry and Physics of Lipids

journal homepage: www.elsevier.com/locate/chemphyslip

AFM study of the interaction of cytochrome P450 2C9 with phospholipid bilayers

Matthew R. Nussio[a], Nicolas H. Voelcker[a], John O. Miners[b], Benjamin C. Lewis[b], Matthew J. Sykes[b], Joseph G. Shapter[a,*]

[a] School of Chemistry, Physics and Earth Sciences, Flinders University, Sturt Road, Bedford Park, Adelaide, SA 5001, Australia
[b] Department of Clinical Pharmacology, Flinders University, Sturt Road, Bedford Park, Adelaide, SA 5001, Australia

ARTICLE INFO

Article history:
Received 19 March 2009
Received in revised form 7 August 2009
Accepted 9 November 2009
Available online 17 November 2009

Keywords:
Cytochrome P450
Membrane protein
Phospholipid bilayers
Atomic force microscopy (AFM)

ABSTRACT

Cytochromes P450 (CYP) are key enzymes involved in the metabolism of drugs and other lipophilic xenobiotics and endogenous compounds. In this study, atomic force microscopy was applied to characterise the association of CYP2C9 to dimyristoylphosphatidylcholine (DMPC) supported phospholipid bilayers. CYP2C9 was found to exclusively localise in the gel domains of partially melted DMPC bilayers. Despite lacking the N-terminus transmembrane spanning domain, the CYP2C9 protein appeared to partially embed into the membrane bilayer, as evidenced by an increase in melting temperature of surrounding phospholipids. Reversible binding of CYP2C9 via an engineered His tag to a phospholipid bilayer was facilitated using nickel-chelating lipids, presenting potential applications for biosensor technologies.

1. Introduction

Membrane proteins constitute the largest fraction by weight of most cellular membranes (Tien and Ottova, 2001). They play a pivotal role in many cellular processes, for example, energy transfer, cell homeostasis, signal transduction and cell communication, and hence are highly relevant to human physiology and disease. The ability to understand the structure and function of membrane proteins relies on our capacity to design experimental systems mimicking their native environment (Milhiet et al., 2006; Stahlberg et al., 2001a; Torres et al., 2003). The function of many membrane proteins is also susceptible to variations in membrane composition and phase. The basic strategy of reconstituting proteins into liposomes to form proteoliposomes has been used as a powerful approach to investigate many membrane proteins in a controlled environment (Kumar et al., 2007; MirAfzali et al., 2005; Puttner et al., 1989; Zhao et al., 1999).

The P450s comprise a superfamily of heme-thiolate proteins that catalyse the mono-oxygenation of a myriad of compounds, including drugs, environmental chemicals and endogenous compounds. The human genome contains 57 functional *CYP* genes and 58 pseudogenes (Guengerich, 2008). Approximately 17 human P450 genes classified in families 1, 2 and 3 encode proteins that metabolise drugs and non-drug xenobiotics (Guengerich, 2008). Drug metabolising P450s are localised to the membrane of the endoplasmic reticulum (ER), with the majority of the protein protruding into the cytosol. The association of the P450 with the phospholipid bilayer is believed to be important for anchoring to the ER membrane and maintaining the correct orientation of the protein for efficient electron transfer from its redox partner, NADPH cytochrome P450 oxidoreductase. An N-terminal signal peptide of mammalian microsomal P450s targets the protein for translocation through the ER, and a single transmembrane helix is presumed to span the phospholipid bilayer (Williams et al., 2000). Although P450 proteins engineered for expression in *Escherichia coli* lack the N-terminal signal peptide and transmembrane spanning domain, they still associate with the membrane and retain catalytic activity (Johnson et al., 2005; Williams et al., 2000).

CYP2C9 is recognised as one of the most important drug metabolising P450s in humans (Miners and Birkett, 1998; Rettie and Jones, 2005; Sykes et al., 2008). In particular, CYP2C9 catalyses the oxidative biotransformation of numerous angiotensin II receptor antagonists (Yasar et al., 2001), coumarin anticoagulants (Au and Rettie, 2008), non-steroidal anti-inflammatory agents (Miners and Birkett, 1998; Miners et al., 1996) and oral hypoglycaemics (Kirchheiner et al., 2005). Additionally, CYP2C9 contributes to the metabolic clearance of drugs from numerous other therapeutic classes, including certain anticonvulsants (Tassaneeyakul et al., 1992), antiasthmatics (Gimm et al., 1996), diuretics (Miners et al., 1995) and statins (Fischer et al., 1999).

Supported phospholipid bilayers (SPBs) are becoming increasingly popular for the study of membrane related processes *in vitro*. In particular, SPBs have been used to characterise membrane structure (Chiantia et al., 2006; Domenech et al., 2007, 2006b),

* Corresponding author. Tel.: +61 8 8201 2005; fax: +61 8 8201 2905.
E-mail address: joe.shapter@flinders.edu.au (J.G. Shapter).

0009-3084/$ – see front matter © 2009 Elsevier Ireland Ltd. All rights reserved.
doi:10.1016/j.chemphyslip.2009.11.003

drug–membrane interactions (Berquand et al., 2004; Leonenko et al., 2006; Montero et al., 2006; Nussio et al., 2007) and protein–membrane interactions (Merino-Montero et al., 2006; Mueller et al., 2000). The incorporation of a thin lubricating layer of water between the SPB and the substrate provides the bilayer with flexibility and fluidity, creating a dynamic system where lipid molecules can diffuse laterally (Reimhult et al., 2003; Sackmann, 1996). Proteoliposome rupture and fusion into SPBs gives rise to proteolipid layers which offer suitable biomimetic lipid interfaces that preserve protein function, are amenable to characterisation by atomic force microscopy (AFM) and, due to their long term stability, are suitable for use in biosensor devices (Cornell et al., 1997).

AFM represents an attractive technique for the analysis of biological structures. Notably, it has been demonstrated that AFM has the ability to provide high-resolution surface topology images of biological membranes and thus resolve membrane domains and phases (Domenech et al., 2006a, 2006b; Nussio et al., 2008; Reviakine et al., 2000). AFM has also been employed to investigate the structure, assembly and oligomeric state of membrane proteins. For example, AFM has been used to characterise the structure of membrane-embedded rotors of bacterial Na^+-ATP synthase (Stahlberg et al., 2001b), the assembly of photosynthetic complexes in their native environment (Scheuring and Sturgis, 2005) and the native oligomeric arrangement of the G protein-coupled receptor, rhodopsin (Fotiadis et al., 2003).

Here we report an AFM investigation of the interaction of cytochrome P450 (CYP2C9) with SPBs. This study characterised the association of CYP2C9 protein, which lacked the N-terminal signal peptide and transmembrane spanning domain, with a synthetic lipid bilayer and examined the effects of protein association on domain phase. As CYP2C9 was engineered with a 6×histidine (6×His) tag, experiments also immobilised the protein to a Ni^{2+}-nitrilotriacetate (NTA)-lipid containing bilayer, resulting in association of monomeric protein. This approach may have potential applications in biosensor devices.

2. Materials and methods

2.1. Chemicals

1,2-Dimyristoyl-*sn*-glycero-3-phosphatidylcholine (DMPC) and 1,2-dioleoyl-*sn*-glycero-3-[(N-(5-amino-1-carboxypentyl)iminodiacetic acid)succinyl] (nickel salt) (DOGS-NTA-Ni^{2+}) were purchased from Avanti Polar Lipids (Birmingham, AL); HEPES ≥ 99%, sodium cholate, dithiothreitol ≥99% were purchased from Sigma–Aldrich (Sydney, Australia). All other chemicals were of the highest commercial quality available and were used without further purification. All aqueous solutions were prepared with Milli-Q grade reagent water with resistance ≈18.2 MΩ. Aqueous solutions were also filtered through a 0.2 μm membrane filter.

2.2. Expression and purification of CYP2C9

The expression and isolation of human CYP2C9 has been described in detail elsewhere (Johnson et al., 2005). Briefly, the CYP2C9 cDNA was modified for expression in *E. coli* by replacing the second codon with GCT (which codes for Ala), deleting codons 3–20, and adjusting codons 21–26 for bacterial codon bias. In addition, a 6×histidine (6×His) tag was added to the C-terminus to facilitate protein purification by column chromatography (Ni-NTA agarose beads). SDS-PAGE of the isolated protein exhibited a single band when probed separately with anti-CYP2C9 and anti-His antibodies (Fig. 1), and catalytic activity was demonstrated with the prototypic CYP2C9 substrates, diclofenac and torsemide (Johnson et al., 2005).

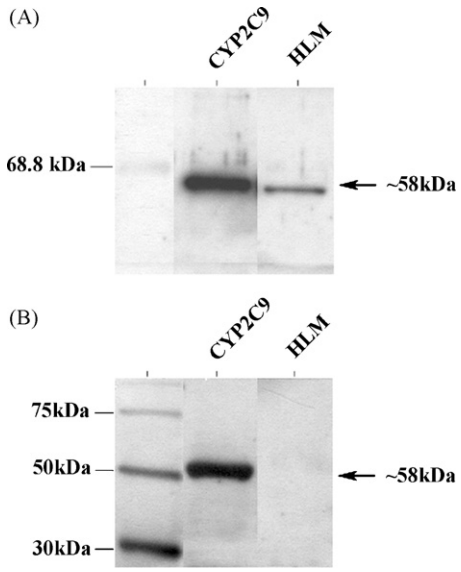

Fig. 1. Western blot of purified His-tagged CYP2C9 probed with anti-CYP2C9 (panel A) and anti-His (panel B) primary antibodies. The sample contained 1 μg of purified protein. Human liver microsomes (HLM; 10 μg) were used as the control.

2.3. Vesicle preparation and protein reconstitution

2.3.1. Cholate dialysis (CD) method using single components

Vesicular reconstitution of CYP2C9 was performed by cholate dialysis (CD), as described elsewhere (Reed et al., 2006; Taniguchi et al., 1979). Briefly, aliquots of lipid were first dissolved in chloroform/methanol (3:1, v:v), followed by evaporation of the solvent under nitrogen. Lipid samples were further dried under vacuum for 2 h prior to being suspended in 10 mM HEPES 150 mM NaCl (pH 7.2) containing 1% sodium cholate solution. Lipid concentrations ranged from 100 μM to 1 mM DMPC. CYP2C9 was then added to a final concentration of 60 nM. The samples were then immediately transferred to 0.5 to 3 mL Slide-a-Lyzer cassettes (Pierce Chemical, Rockford, IL) and dialysed at 4 °C for 36 h with three exchanges (12 h each) of 3 L of dialysis buffer containing 10 mM HEPES buffer with 150 mM NaCl (pH 7.2) and 0.1 mM dithiothreitol. This was done to remove the sodium cholate. Resultant large unilamellar vesicles (LUVs) containing CYP2C9 were then subjected to extrusion (Avanti Mini-Extruder, Avanti Polar Lipids, Birmingham, AL) to give small unilamellar vesicles (SUVs) of well defined size, typically 100 nm. In preparation of SPBs, 4 mM $CaCl_2$ was added to final lipid/protein SUV solutions.

2.3.2. Formation of vesicles containing NTA-Ni lipids for protein reconstitution

Multilamellar vesicles (MLVs) were prepared by first dissolving aliquots of DMPC and DOGS-NTA-Ni lipids (4:1) in chloroform/methanol (3:1 v:v), followed by evaporation of the solvent under nitrogen. Lipid samples were further dried under vacuum for 2 h prior to being suspended in 10 mM HEPES buffer with 150 mM NaCl 4 mM $CaCl_2$ (pH 7.2). The final total concentration of lipids was 1 mM. Samples were then sonicated for 30 min in an Elma S30H Elmasonic bath sonicator. Sonication ensures MLVs are converted into LUVs which when subjected to extrusion give SUVs of well defined size.

2.3.3. AFM imaging

The imaging of SPBs was performed using a commercial AFM (Nanoscope IV, Digital Instruments, Veeco, Santa Barbara, CA). All images were obtained by means of *in situ* tapping™ mode using triangular Si_3N_4 cantilevers (Digital Instruments, Veeco)

which had a nominal spring constant of 0.15 N m^{-1}. Formation of SPBs was achieved by depositing 100 μL of 100 nm SUV solution onto a freshly cleaved mica surface. Prepared surfaces were then incubated at temperatures greater than their gel–fluid phase transition temperature (T_M) for 2 h to promote SPB formation. Prior to imaging, bilayer surfaces were washed five times with a buffer containing no lipid or calcium salt.

3. Results and discussion

3.1. CYP 2C9 reconstitution

Initial studies investigated the surface topography of SPBs formed using pure DMPC vesicles as well as DMPC vesicles containing CYP2C9 prepared by the CD method. At temperatures close to 20 °C, the SPB appeared to be partially melted (Fig. 2). Previous studies investigating the effects of temperature on DMPC bilayers have demonstrated decoupling of the top and bottom leaflets (Feng et al., 2005; Garcia-Manyes et al., 2005). The measured height difference between the upper and lower domains was 0.44 ± 0.07 nm and was consistent with the top leaflet of the bilayer being partially melted (Feng et al., 2005; Tokumasu et al., 2003). Upper and lower domains corresponded to gel (L_β) and liquid-crystalline (L_α) lamellar phases, respectively. Phase imaging was also employed to confirm the lamellar phases in the top leaflet, as the phase lag of the tip relative to the excitation signal is sensitive to surface properties, such as adhesion and viscoelasticity. Fig.2A (phase image) clearly demonstrates a large phase contrast (∼1°) between the two domains, which is interpreted as a change in bilayer softness (Evans, 2008; Leonenko et al., 2000), and thus confirms the proposed lamellar phases on the top leaflet of the DMPC bilayer.

Reconstitution of CYP2C9 in DMPC vesicles by CD provides a lipid environment that simulates that of the ER membrane since the protein associates with a unilamellar bilayer (Reed et al., 2006). Cholate solubilises the CYP within the lipid matrix and, upon removal of the detergent by dialysis, the lipids form unilamellar vesicles with the CYP2C9 protein incorporated, that is proteoliposomes (Ingelman-Sundberg and Glaumann, 1980; Reed et al., 2006; Taniguchi et al., 1979). Upon exposure to a flat planar substrate such as mica, the proteoliposomes adhere, rupture and spread to form a continuous SPB (see Fig. 2(ii)). Imaging of the reconstituted CYP2C9-bilayer may then be performed using AFM. As contact mode can often damage and/or push flexible small biomolecules along the surface, all experiments were performed using tapping mode to best maintain the structural integrity of the CYP2C9 protein.

The clear changes in morphology compared to experiments performed without the protein reconstituted (Fig. 2A) suggest successful reconstitution of CYP2C9 (Fig. 2B). Simultaneous phase imaging also demonstrated a contrast between protrusions (such as those circled in Fig. 2B) and the bilayer environment, further indicating association of CYP2C9 with the membrane (Fig. 2B). The protrusions were 1.73 ± 0.41 nm high and 60–80 nm in diameter (n = 100). Based on the human CYP2C9 crystal structure (Wester et al., 2004), the height and width of monomeric proteins are approximately 6 and 4 nm, respectively. Experiments utilising AFM are subject to tip-induced broadening effects that overestimate the lateral dimensions of biomolecules (Bustamante et al., 1992). Previous studies utilising AFM have observed diameters on the order of 15–20 nm for monomeric CYP proteins (Gannett et al., 2006; Kiselyova et al., 1999). It would therefore appear that CYP2C9 was not in the monomeric form. Consistent with the current study, however, previous measurements performed with AFM have also demonstrated the heights of P450 molecules to be low compared to the dimensions obtained from crystal structures (Bayburt and Sligar, 2002; Kiselyova et al., 1999; Kuznetsov et al., 2004).

As AFM imaging can distort the height of flexible membrane-associated proteins, previous work performed by Bayburt and Sligar (2002) utilised force-distance measurements to assess the height of CYP2B4 molecules more accurately. A measured height of ∼3.5 nm was then used to develop a model for the interaction of CYP with the membrane surface. The model suggested the protein sits upright, with both proximal and distal faces normal to the bilayer (Bayburt and Sligar, 2002). In the native state, a single transmembrane helix anchors the CYP to the phospholipid bilayer (Johnson, 2003; Vergères et al., 1989). As the transmembrane domain comprises hydrophobic amino acids, its presence increases protein aggregation and reduces solubility (Johnson, 2003). For these reasons, expressed P450s lack this transmembrane spanning domain, and the transmembrane domain is therefore omitted in the model depicted by Bayburt and Sligar. In addition to the work of Bayburt and Sligar, several other studies have also demonstrated the ability of microsomal CYPs to retain their membrane localisation in the absence of the transmembrane spanning domain (Bayburt and Sligar, 2002; Cosme and Johnson, 2000; Cullin, 1992; Larson et al., 1991a, 1991b; Pernecky et al., 1993; Sagara et al., 1993). These membrane interactions, however, were easily dissociated under high salt buffer conditions (Cosme and Johnson, 2000). Hydrophobic residues between F and G helices, in close proximity to the transmembrane spanning domain, are believed to represent the portion of the P450 protein that associates with the membrane bilayer (De Lemos-Chiarandini et al., 1987; Johnson, 2003; Williams et al., 2000). Of significant interest, the proposed orientation of the protein also provides access for hydrophobic substrates to enter the enzymes catalytic site from the vicinity of the membrane (Williams et al., 2000).

3.2. Localisation of reconstituted CYP2C9

An interesting observation for DMPC bilayers reconstituted with CYP2C9 is the location of the protein aggregates. CYP2C9 protein is exclusively located within the L_β domains of the SPB. The accumulation of the protein on the higher L_β domains, as opposed to the surrounding L_α domains, suggests that the CYP either has preference for a L_β environment or the incorporation into the membrane influences the lipid bilayer properties. Previous studies utilising AFM have demonstrated that placental alkaline phosphatase preferentially partitions into L_β domains (Chiantia et al., 2006). Studies of the interaction of the first 42 residues of β-amyloid peptides with SPBs have also demonstrated a preferential interaction with L_β domains, although reconstitution of these peptides revealed aggregates randomly distributed in both the L_β and L_α phase domains (Choucair et al., 2007). It is also known that glycosylphosphatidylinositol (GPI)-anchored proteins partition into lipid rafts, while many transmembrane proteins are located in non-raft phases (Sieber et al., 2007). In addition, it has been shown that the exact location of the membrane species is very sensitive to the chemical nature of the both the lipid and the protein or peptide (Planque et al., 1999). Proteins can also be confined to a specific region of the microdomain if the activation energy of crossing the domain barrier is larger than the kinetic energy of the protein itself (Vereb et al., 2003). In general, membrane proteins appear to preferentially locate into different membrane phases, dependent on the lipid packing behaviour of the bilayer phospholipids.

3.3. Effects of reconstituted CYP2C9 on the local phospholipid environment

As DMPC has a transition temperature close to room temperature (T_M ∼ 23 °C), subtle changes in temperature can affect

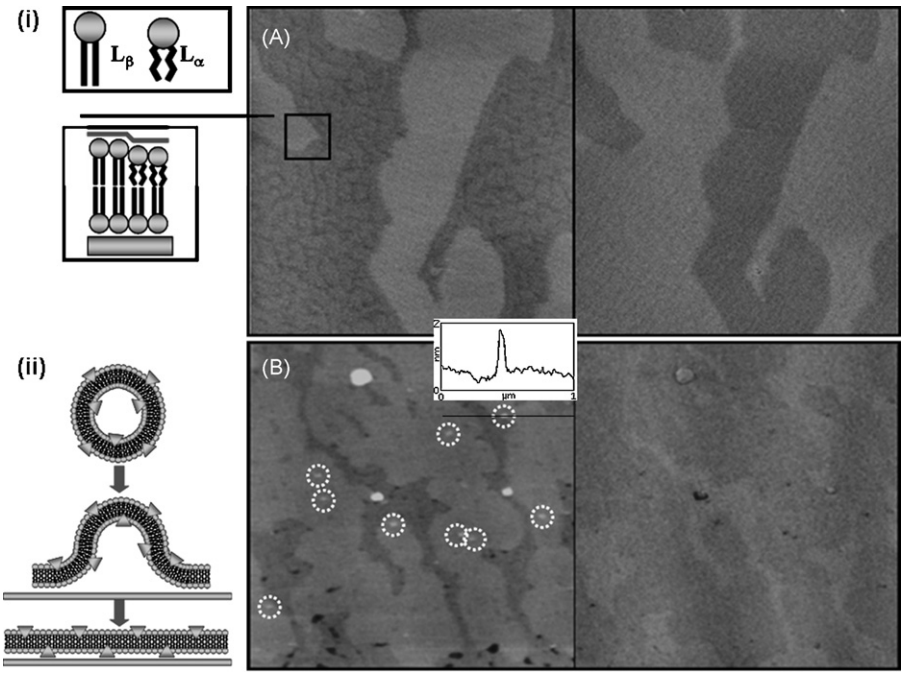

Fig. 2. (A) Height (left; *Z*-scale: 5 nm) and phase (right; *Z*-scale: 10°) AFM images (2.5 × 2.5 μm^2; 512 lines × 512 lines) of a DMPC supported phospholipid bilayer (pH 7.2). L_β extend 0.44 nm ± 0.07 nm above surrounding L_α domain. Schematic (i): models of supported phospholipid bilayers showing partial melting of the upper bilayer leaflet. (B) Height (left; *Z*-scale: 5 nm) and phase (right; *Z*-scale: 10°) AFM images (2.5 × 2.5 μm^2; 512 lines × 512 lines) of a DMPC supported phospholipid bilayer with CYP2C9 reconstituted (pH 7.2). All CYP2C9 protein molecules were exclusively located on the L_β domains (circled). Schematic (ii): proteoliposome rupture and fusion into SPBs gives rise to proteolipid layers for the visualisation by AFM.

the phase of the bilayer membrane. We observed an effect of CYP2C9 on the melting behaviour of L_β domains with increasing temperature (Fig. 3). Typically, the most energetically favourable process of melting occurs at the interface between the L_β and L_α domains, decreasing the size of the L_β domains towards the centre of the domain. However, the localisation of CYP2C9 in L_β domains increases the melting temperature of neighbouring phospholipid molecules, causing the final region of melting to occur at locations in close proximity with the reconstituted protein. Consistent with this observation, it has been known for some time that phospholipids in the vicinity of microsomal P450s are more highly organised than in the remainder of the membrane (Stier and Sackmann, 1973). The association of CYP2C9 into distinct L_β lipid domains clearly demonstrates the influence of this protein on the T_M of phospholipid bilayers. Since the transmembrane spanning domain is absent, the observed melting behaviour highlights the ability of CYP2C9 to interact with the membrane, presumably by its hydrophobic domain.

3.4. Binding of CYP2C9 to nickel-chelating lipids

As the *E. coli* expressed CYP2C9 incorporated a 6×His tag at the C-terminus, nickel-chelating lipids (DOGS-NTA-Ni^{2+}) were also used to bind CYP2C9 to phospholipid bilayers. This method has been utilised for the specific binding of proteins and peptides in previous studies (Celia et al., 1999; Kienberger et al., 2001; Lud et al., 2006; Prachayasittikula et al., 2005). As employed in protein purification, binding occurs due to an interaction between the Ni^{2+}-NTA headgroups and the His tag of the protein. The specific binding of the 6×His tag anchors the protein to the membrane, forming a non-covalent complex. This process is reversible as addition of a chelator for Ni^{2+}, such as EDTA, displaces the His-tagged protein.

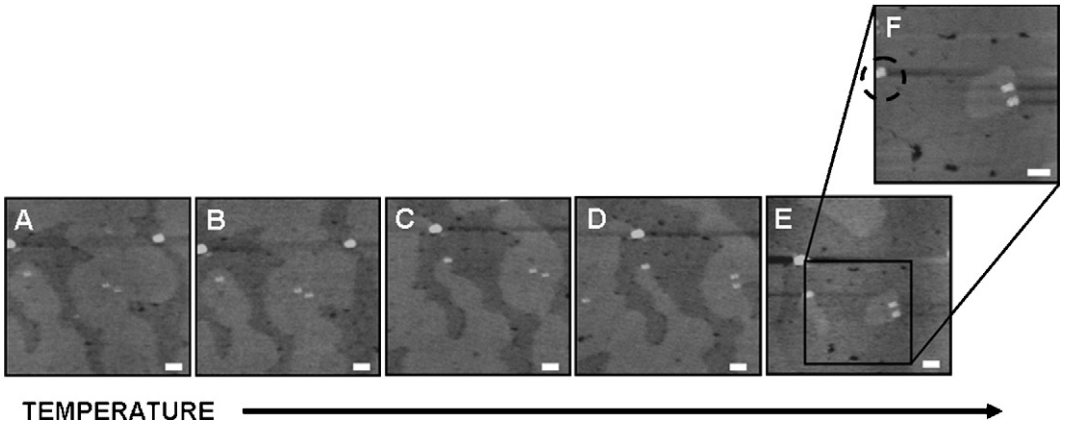

Fig. 3. AFM topographic images of DMPC supported phospholipid bilayers with CYP2C9 reconstituted (pH 7.2). Small changes in temperature (~1°C) melt the L_β domains (A–F). CYP2C9 appears to stabilise L_β domains, causing the final region of melting to occur at locations surrounding the protein (F, circled region). Scale bars: 200 nm, *Z*-scale: 5 nm, 512 lines × 512 lines. The images were taken over a 50 min period.

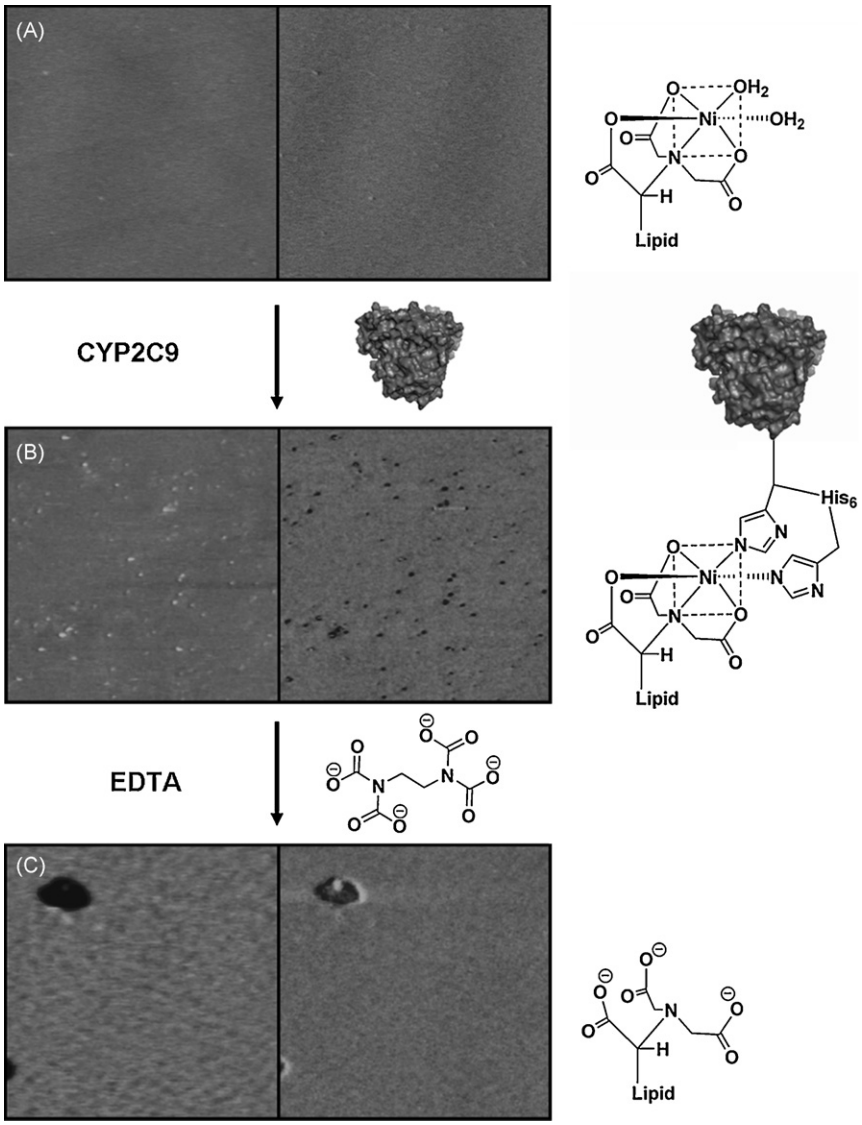

Fig. 4. Height (left; *Z*-scale: 5 nm) and phase (right; *Z*-scale: 10°) AFM images (2.0 × 2.0 μm^2; 512 lines × 512 lines) of DMPC:DOGS-NTA-Ni^{2+} (4:1) phospholipid bilayers, (A) prior to CYP2C9 interaction, (B) with CYP2C9 bound, and (C) after addition of 4 mM EDTA. Schematic of CYP2C9 binding: specific binding of the His tag anchors the protein to the membrane, forming a non-covalent complex. Addition of EDTA facilitates the unbinding of the His tag, removing the protein from the phospholipid bilayer.

Fig.4 shows the reversible binding of CYP2C9 to phospholipid bilayers comprising DOGS-NTA-Ni^{2+} lipids incorporated in a matrix of DMPC.

Initial experiments investigated the surface topology of DMPC:DOGS-NTA-Ni^{2+} (4:1) prior to CYP2C9 interaction (Fig. 4A). In contrast to work presented in Fig. 2A, SPBs did not demonstrate any noticeable lamellar phase separation, and it is assumed that DOGS-NTA-Ni^{2+} lowered the T_M of neighbouring DMPC phospholipids since the transition temperature of DOGS should be well below that of DMPC given that the transition temperature of the phosphatidylcholine with the same aliphatic chain (1,2-dioleoyl-*sn*-glycero-3-phosphatidylcholine) has a transition temperature of −20 °C. After moving the AFM tip away from the sample, the DMPC:DOGS-NTA-Ni^{2+} bilayer was then exposed to a 0.7 nM solution of CYP2C9. After 5 min, the sample was rinsed thoroughly and the tip was reengaged. Upon incorporation of CYP2C9 into the DMPC:DOGS-NTA-Ni^{2+} phospholipid bilayers, protrusions 1.60 ± 0.53 nm high and 15–20 nm wide were observed (Figs. 4B and 5). Extensive washing of the membrane did not remove the CYP2C9 from the bilayer. Consistent with previous results shown in Fig. 2 for the one component membrane, simultaneous phase imaging demonstrated a disparity between the CYP2C9 protein and the bilayer environment. This disparity confirms that the protrusions observed for the bilayer containing the NTA-Ni^{2+} were due to presence of protein. However, in contrast to observations with reconstituted CYP2C9 (Fig. 2B), monomeric protein with lateral dimensions comparable to previous AFM studies was detected (Gannett et al., 2006; Kiselyova et al., 1999). The different binding is expected as the nickel-chelating agent will bind strongly with the His tags of the protein but will only be able to bond to one protein giving monomeric binding. The protein distribution also appeared to be random, confirming a uniform mixing of the two phospholipids. Previous attempts in this lab to bind CYP2C9 to a preformed DMPC membrane bilayer in the absence of nickel-chelating lipids have been unsuccessful and thus no other protein aggregates adsorbed to DMPC such as those shown in the single component SPB (Fig. 2B), where the proteins are incorporated at the vesicle stage, are observed. Typically used for protein purification, the Ni^{2+}-NTA head group facilitates the monomeric binding of CYP2C9 as visualised by AFM. Finally, displacement of CYP2C9 was achieved after incubation of the bilayer in 4 mM EDTA (Fig. 4C), a chelator of Ni^{2+}, for 5 min. The exposure to EDTA solution required

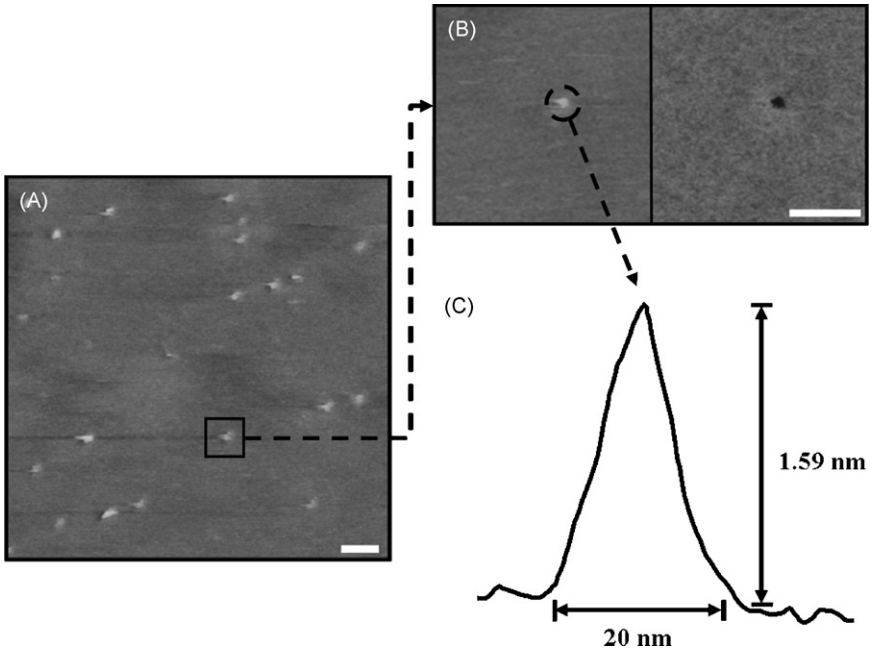

Fig. 5. (A) AFM topographic image of DMPC:DOGS-NTA-Ni2+ (4:1) phospholipid bilayers with CYP2C9 bound. (B) Topographic height (left, *Z*-scale: 5 nm) and phase (right, *Z*-scale: 10°) image zoom of CYP2C9 binding via 6×His tag. Scale bars: 100 nm. (C) Cross-sectional analysis of CYP2C9 protrusions yielded a height of 1.60 nm ± 0.53 nm and diameters of 15–20 nm.

removal of the sample from the AFM meaning that different areas of the bilayers are being imaged in Fig. 4A and C.

The use of the Ni^{2+}-NTA group in the lipid bilayer could potentially be used to probe targeted single proteins interactions with bilayers. The moiety allows the reliable isolation of target proteins and indeed the density of such species can be changed by modifying the relative amount lipid with the chelating agent attached. This could for example allow examination of the functionality of isolated proteins as opposed to aggregated proteins. Thus the importance of protein clusters could be examined. Isolation of the individual proteins will potentially also contribute to knowledge of protein and perhaps even sub-protein structure in an environment similar to the protein's normal physiological environment.

4. Conclusion

AFM was employed to investigate the association of CYP2C9 with a synthetic membrane bilayer. It was demonstrated that CYP2C9 was exclusively localised in the L_β domains of phase separated DMPC SPB. Upon melting of the L_β domains, the final region of melting occurred at locations surrounding the protein. Thus, it may be concluded that CYP2C9 increases the melting temperature of neighbouring phospholipid molecules as it partially embeds into the membrane bilayer. As CYP2C9 was lacking its transmembrane spanning domain, the protein was presumably associated with the membrane by its hydrophobic domain and this provides the basis for the altered 'local' membrane stability of neighbouring phospholipids.

The reversible binding of the His-tagged CYP2C9 to nickel-chelating lipids was observed. This system constitutes a suitable interface to mimic membrane behaviour, as it comprises an artificial bilayer that has the ability to bind a range of integral membrane proteins. As monomeric CYP2C9 protein was immobilised, it is possible that the system may have potential applications in biosensor technologies for assessing the role of individual P450s, and indeed other enzymes, in the metabolism of newly discovered drugs.

Acknowledgement

This work is supported by the Australian Microscopy and Microanalysis Research Facility (AMMRF).

References

Au, N., Rettie, A.E., 2008. Pharmacogenomics of 4-hdroxycoumarin anticoagulants. Drug Metabolism Reviews 40, 355–375.
Bayburt, T.H., Sligar, S.G., 2002. Single-molecule height measurements on microsomal cytochrome P450 in nanometer-scale phospholipid bilayer disks. Proceedings of the National Academy of Sciences 99, 6725–6730.
Berquand, A., Mingeot-Leclerq, M.P., Dufrêne, Y.F., 2004. Real-time imaging of drug–membrane interactions by atomic force microscopy. Biochimica et Biophysica Acta 1664, 198–205.
Bustamante, C., Vesenka, J., Tang, C.L., Rees, W., Guthold, M., Kellers, R., 1992. Circular DNA molecules imaged in air by scanning force microscopy. Biochemistry 31, 22–26.
Celia, H., Wilson-Kubalek, E., Milligan, R.A., Teyton, L., 1999. Structure and function of a membrane-bound murine MHC class I molecule. Proceedings of the National Academy of Sciences 96, 5634–5639.
Chiantia, S., Ries, J., Kahya, N., Schwille, P., 2006. Combined AFM and two-focus SFCS study of raft-exhibiting model membranes. ChemPhysChem 7, 2409–2418.
Choucair, A., Chakrapani, M., Chakravarthy, B., Katsaras, J., Johnston, L.J., 2007. Preferential accumulation of $A((1-42)$ on gel phase domains of lipid bilayers: an AFM and fluorescence study. Biochimica et Biophysica Acta 1768, 146–154.
Cornell, B.A., Braach-Maksvytis, V.L.B., King, L.G., Osman, P.D.J., Raguse, B., Wieczorek, L., Pace, R.J., 1997. A biosensor that uses ion-channel switches. Nature 387, 580–583.
Cosme, J., Johnson, E.F., 2000. Engineering microsomal mytochrome P450 2C5 to me a moluble, monomeric enzyme. The Journal of Biological Chemistry 275, 2545–2553.
Cullin, C., 1992. Two distinct sequences control the targeting and anchoring of the mouse P450 1A1 into the yeast endoplasmic reticulum membrane. Biochemical and Biophysical Research Communications 184, 1490–1495.
De Lemos-Chiarandini, C., Frey, A.B., Sabatini, D.D., Kreibich, G., 1987. Determination of the membrane topology of the phenobarbital-inducible rat liver cytochrome P-450 isoenzyme PB-4 using site-specific antibodies. The Journal of Cell Biology 104, 209–219.
Domenech, O., Merino-Montero, S., Montero, M.T., Hernandez-Borrell, J., 2006a. Surface planar bilayers of phospholipids used in protein membrane reconstitution: an atomic force microscopy study. Colloids and Surfaces B: Biointerfaces 47, 102–106.
Domenech, O., Morros, A., Cabanas, M.E., Montero, M.T., Hernandez-Borrell, J., 2007. Supported planar bilayers from hexagonal phases. Biochimica et Biophysica Acta 1768, 100–106.
Domenech, O., Sanz, F., Montero, M.T., Harnandez-Borrell, J., 2006b. Thermodynamic and structural study of the main phospholipid components comprising

the mitochondrial inner membrane. Biochimica et Biophysica Acta 1758, 213–221.
Evans, K.O., 2008. Supported phospholipid bilayer interaction with components found in typical room-temperature ionic liquids—a QCM-D and AFM study. International Journal of Molecular Sciences 9, 498–511.
Feng, Z.V., Spurlin, T.A., Gewirth, A.A., 2005. Direct visualization of asymmetric behaviour in supported lipid bilayers at the gel–fluid phase transition. Biophysical Journal 88, 2154–2164.
Fischer, V., Johanson, L., Heitz, F., Tullman, R., Graham, E., Baldeck, J.-P., Robinson, W.T., 1999. The 3-hydroxy-3-methylglutaryl coenzyme A reductase inhibitor fluvastatin: effect of human cytochrome P450 and implications for metabolic drug interactions. Drug Metabolism and Disposition 27, 410–416.
Fotiadis, D., Liang, Y., Filipek, S., Saperstein, D.A., Engel, A., Palczewski, K., 2003. Atomic-force microscopy: rhodopsin dimers in native disc membranes. Nature 421, 127–128.
Gannett, P.M., Kabulski, J., Perez, F.A., Liu, Z., Lederman, D., Locuson, C.W., Ayscue, R.R., Thomsen, N.M., Tracy, T.S., 2006. Preparation, characterization and substrate metabolism of gold-immobilized cytochrome P450 2C9. Journal of American Chemical Society 128, 8374–8375.
Garcia-Manyes, S., Oncins, G., Sanz, F., 2005. Effect of temperature on the nanomechanics of lipid bilayers studied by force spectroscopy. Biophysical Journal 89, 4261–4274.
Gimm, S.W., Stams, K.R., Aaron, E.J., 1996. Zafirlukast is a substrate for CYP2C9 and an inhibitor of CYP2C9 and CYP3A. International Society for the Study of Xenobiotics Processings 10, 392.
Guengerich, F.P., 2008. Cytochrome P450 and chemical toxicology. Chemical Research in Toxicology 21, 70–83.
Ingelman-Sundberg, M., Glaumann, H., 1980. Incorporation of purified components of the rabbit liver microsomal hydroxylase system into phospholipid vesicles. Biochimica et Biophysica Acta 599, 417–435.
Johnson, D.L., Lewis, B.C., Elliot, D.J., Miners, J.O., Martin, L.L., 2005. Electrochemical characterisation of human cytochrome P450 CYP2C9. Biochemical Pharmacology 69, 1533–1541.
Johnson, E.F., 2003. Deciphering substrate recognition by drug-metabolizing cytochromes P450. Drug Metabolism and Disposition 31, 1532–1540.
Kienberger, F., Moser, R., Schindler, H., Blass, D., Hinterdorfer, P., 2001. Quasi-crystalline arrangement of human rhinovirus 2 on model cell membranes. Single Molecules 2, 99–103.
Kirchheiner, J., Roots, I., Goldammer, M., Rosenkranz, B., Brockmöller, J., 2005. Effect of genetic polymorphisms in cytochrome P450 (CYP) 2C9 and CYP2C8 on the pharmacokinetics of oral antidiabetic drugs. Clinical Pharmacokinetics 44, 1209–1225.
Kiselyova, O.I., Yaminsky, I.V., Ivanov, Y.D., Kanaeva, I.P., Kuznetsov, V.Y., Archakov, A.I., 1999. AFM study of membrane proteins, cytochrome P450 2B4, and NADPH-cytochrome P450 reductase and their complex formation. Archives of Biochemistry and Biophysics 371, 1–7.
Kumar, A., Tyagi, N.K., Arevalo, E., Miller, K.W., Kinne, R.K.H., 2007. A proteomic study of sodium/d-glucose cotransporter 1 (SGLT1): topology of loop 13 and coverage of other functionally important domains. Biochimica et Biophysica Acta (BBA)—Proteins & Proteomics 1774, 968–974.
Kuznetsov, V.Y., Ivanov, Y.D., Archakov, A.I., 2004. Atomic force microscopy revelation of molecular complexes in the multiprotein cytochrome P450 2B4-containing system. Proteomics 4, 2390–2396.
Larson, J.R., Coon, M.J., Porter, T.D., 1991a. Alcohol-inducible cytochrome P-450IIE1 lacking the hydrophobic NH_2-terminal segment retains catalytic activity and is membrane-bound when expressed in *Escherichia coli*. The Journal of Biological Chemistry 266, 7321–7324.
Larson, J.R., Coon, M.J., Porter, T.D., 1991b. Purification and properties of a shortened form of cytochrome P-450 2E1: deletion of the NH_2-terminal membrane-insertion signal peptide does not alter the catalytic activities. Proceedings of the National Academy of Sciences 88, 9141–9145.
Leonenko, Z., Finot, E., Cramb, D., 2006. AFM study of interaction forces in supported planar DPPC bilayers in the presence of general anesthetic halothane. Biochimica et Biophysica Acta 1758, 487–492.
Leonenko, Z.V., Carnini, A., Cramb, D.T., 2000. Supported planer bilayer formation by vesicle fusion: the interaction of phospholipid vesicles with surfaces and the effect of gramicidin on bilayer properties using atomic force microscopy. Biochimica et Biophysica Acta 1509, 131–147.
Lud, S.Q., Nikolaides, M.G., Haase, I., Fischer, M., Bausch, A.R., 2006. Field effect of screened charges: electrical detection of peptides and proteins by a thin-film resistor. ChemPhysChem 7, 379–384.
Merino-Montero, S., Domenech, O., Montero, M.T., Hernandez-Borrell, J., 2006. Preliminary atomic force microscopy study of two-dimensional crystals of lactose permease from *Escherichia coli*. Biophysical Chemistry 119, 78–83.
Milhiet, P.-E., Gubellini, F., Berquand, A., Dosset, P., Rigaud, J.-L., 2006. High-resolution AFM of membrane proteins directly incorporated at high density in planar lipid bilayer. Biophysical Journal 91, 3268–3275.
Miners, J.O., Birkett, D.J., 1998. Cytochrome P4502C9: an enzyme of major importance in human drug metabolism. British Journal of Clinical Pharmacology 45, 525–538.
Miners, J.O., Coulter, S., Tukey, R.H., Veronese, M.E., Birkett, D.J., 1996. Cytochromes P450 1A2 and 2C9 are responsible for the human hepatic O-demethylation of R- and S-naproxen. Biochemical Pharmacology 51, 1003–1008.
Miners, J.O., Rees, D.L.P., Valente, L., Veronese, M.E., Birkett, D.J., 1995. Human hepatic cytochrome P450 2C9 catalyzes the rate-limiting pathway of torsemide metabolism. Journal of Pharmacology and Experimental Therapeutics 272, 1076–1081.
MirAfzali, Z., Leipprandt, J.R., McCracken, J.L., DeWitt, D.L., 2005. Fast, efficient reconstitution of the cyclooxygenases into proteoliposomes. Archives of Biochemistry and Biophysics 443, 60–65.
Montero, M.T., Pijoan, M., Merino-Montero, S., Vinuesa, T., Hernandez-Borrell, J., 2006. Interfacial membrane effects of fluoroquinolones as revealed by a combination of fluorescence binding experiments and atomic force microscopy observations. Langmuir 22, 7574–7578.
Mueller, H., Butt, H., Bamberg, E., 2000. Adsorption of membrane-associated proteins to lipid bilayers studied with an atomic force microscope: myelin basic protein and cytochrome c. Journal of Physical Chemistry B 104, 4552–4559.
Nussio, M.R., Liddell, M., Sykes, M.J., Miners, J.O., Shapter, J.G., 2007. Dynamics of phospholipid membrane growth and drug–membrane interactions probed by atomic force microscopy (AFM). Journal of Scanning Probe Microscopy 2, 41–45.
Nussio, M.R., Voelcker, N.H., Sykes, M.J., McInnes, S.J.P., Gibson, C.T., Lowe, R.D., Miners, J.O., Shapter, J.G., 2008. Lateral heterogeneities in supported bilayers from pure and mixed phosphatidylethanolamine demonstrating hydrogen bonding capacity. Biointerphases 3 (4), 96–104.
Pernecky, S.J., Larson, J.R., Philpot, R.M., Coon, M.J., 1993. Expression of truncated forms of liver microsomal P450 cytochromes 2B4 and 2E1 in *Escherichia coli*: influence of NH_2-terminal region on localization in cytosol and membranes. Proceedings of the National Academy of Sciences 90, 2651–2655.
Planque, M.R.R.d., Kruijtzer, J.A.W., Liskamp, R.M.J., Marshi, D., Greathouse, D.V., Koeppe, R.E., Kruijff Bd, Killian, J.A., 1999. Different membrane anchoring positions of tryptophan and lysine in synthetic transmembrane α-helical peptides. Journal of Biological Chemistry 274, 20839–20846.
Prachayasittikula, V., Isarankura Na Ayudhya, C., Hilterhaus, L., Hinz, A., Tantimongcolwat, T., Galla, H.-J., 2005. Interaction analysis of chimeric metal-binding green fluorescent protein and artificial solid-supported lipid membrane by quartz crystal microbalance and atomic force microscopy. Biochemical and Biophysical Research Communications 327, 174–182.
Puttner, I.B., Sarkar, H.K., Padan, E., Lolkema, J.S., Kaback, H.R., 1989. Characterization of site-directed mutants in the lac permease of *Escherichia coli*. 1. Replacement of histidine residues. Biochemistry 28, 2525–2533.
Reed, J.R., Kelley, R.W., Backes, W.L., 2006. An evaluation of methods for the reconstitution of cytochromes P450 and NADPH P450 reductase into lipid vesicles. Drug Metabolism and Disposition 34, 660–666.
Reimhult, E., Hook, F., Kasemo, B., 2003. Intact vesicle adsorption and supported biomembrane formation from vesicles in solution: influence of surface chemistry, vesicle size, temperature, and osmotic pressure. Langmuir 19, 1681–1691.
Rettie, A.E., Jones, J.P., 2005. Clinical and toxicological relevance of CYP2C9: drug–drug interactions and pharmacogenetics. Annual Review of Pharmacology and Toxicology 45, 477–494.
Reviakine, I., Simon, A., Brisson, A., 2000. Effect of Ca^{2+} on the morphology of mixed DPPC-DOPS supported phospholipid bilayers. Langmuir 16, 1473–1477.
Sackmann, E., 1996. Supported membranes: scientific and practical applications. Science 271, 43–48.
Sagara, Y., Barnes, H.J., Waterman, M.R., 1993. Expression in *Escherichia coli* of functional cytochrome $P450_{c17}$ lacking its hydrophobic amino-terminal signal anchor. Archives of Biochemistry and Biophysics 304, 272–278.
Scheuring, S., Sturgis, J.N., 2005. Chromatic adaptation of photosynthetic membranes. Science 309, 484–487.
Sieber, J.J., Willig, K.I., Kutzner, C., Gerding-Reimers, C., Harke, B., Donnert, G., Rammner, B., Eggeling, C., Hell, S.H., Grubmuller, H., Lang, T., 2007. Anatomy and dynamics of a supramolecular membrane protein cluster. Science 317, 1072–1076.
Stahlberg, H., Fotiadis, D., Scheuring, S., Rémigy, H., Braun, T., Mitsuoka, K., Fujiyoshi, Y., Engel, A., 2001a. Two-dimensional crystals: a powerful approach to assess structure, function and dynamics of membrane proteins. FEBS Letters 504, 166–172.
Stahlberg, H., Müller, D.J., Suda, K., Fotiadis, D., Engel, A., Meier, T., Matthey, U., Dimroth, P., 2001b. Bacterial Na^+-ATP synthase has an undecameric rotor. EMBO Reports 2, 229–233.
Stier, A., Sackmann, E., 1973. Spin labels as enzyme substrates: heterogenous lipid distribution in liver microsomal membranes. Biochimica et Biophysica Acta 311, 400–408.
Sykes, M.J., McKinnon, R.A., Miners, J.O., 2008. Prediction of metabolism by cytochrome P450 2C9: alignment and docking studies of a validated database of substrates. Journal of Medicinal Chemistry 51, 780–791.
Taniguchi, H., Imai, Y., Iyanagi, T., Sato, R., 1979. Interaction between NADPH-cytochrome P-450 reductase and cytochrome P-450 in the membrane of phosphatidylcholine vesicles. Biochimica et Biophysica Acta 550, 341–356.
Tassaneeyakul, W., Veronese, M.E., Birkett, D.J., Doecke, C.J., McManus, M.E., Sansom, L.N., Miners, J.O., 1992. Co-regulation of phenytoin and tolbutamide metabolism in humans. British Journal of Clinical Pharmacology 34, 494–498.
Tien, H.T., Ottova, A., 2001. The lipid bilayer concept and its experimental realization: from soap bubbles, kitchen sink, to bilayer lipid membranes. Journal of Membrane Science 189, 83–117.
Tokumasu, F., Jin, A.J., Feigenson, G.W., Dvorak, J.A., 2003. Atomic force microscopy of nanometric liposome adsorption and nanoscopic membrane domain formation. Ultramicroscopy 97, 217–227.
Torres, J., Stevens, T.J., Samsó, M., 2003. Membrane proteins: the 'Wild West' of structural biology. Trends in Biochemical Sciences 28, 137–144.

Vereb, G., Szollosi, J., Matko, J., Nagy, P., Farkas, T., Vigh, L., Matyus, L., Waldmann, T.A., 2003. Dynamic, yet structured: the cell membrane three decades after the Singer–Nicolson model. Proceedings of the National Academy of Sciences of the Unites States of America 100, 8053–8058.

Vergères, G., Winterhalter, K.H., Richter, C., 1989. Identification of the membrane anchor of microsomal rat liver cytochrome P-450. Biochemistry 28, 3650–3655.

Wester, M.R., Yano, J.K., Schoch, G.A., Yang, C., Griffin, K.J., Stout, C.D., Johnson, E.F., 2004. The structure of human cytochrome P450 2C9 complexed with flurbiprofen at 2.0-Å resolution. The Journal of Biological Chemistry 279, 35630–35637.

Williams, P.A., Cosme, J., Sridhar, V., Johnson, E.F., McRee, D.E., 2000. Mammalian microsomal cytochrome P450 monooxygenase: structural adaptations for membrane binding and functional diversity. Molecular Cell 5, 121–131.

Yasar, U., Tybring, G., Hidestrand, M., Oscarson, M., Ingelman-Sundberg, M., Dahl, M.-L., Eliasson, E., 2001. Role of CYP2C9 polymorphism in losartan oxidation. Drug Metabolism and Disposition 29, 1051–1056.

Zhao, M., Zen, K.-C., Hubbell, W.L., Kaback, H.R., 1999. Proximity between Glu126 and Arg144 in the lactose permease of *Escherichia coli*. Biochemistry 38, 7407–7412.